Comparison Between Nonconforming Movement Methods

O. J. Antunes[1], J. P. A. Bastos[2], N. Sadowski[2], A. Razek[3], L. Santandrea[3], F. Bouillault[3], and F. Rapetti[4]

[1]Centro Federal de Educação Tecnologica de Santa Catarina, Florianopolis, SC, Brazil
[2]Universidade Federal de Santa Catarina, GRUCAD/EEL/CTC, 88040-900 Florianopolis, SC, Brazil
[3]LGEP-UMR 8507 CNRS, Paris VI, Paris XI Univ. and Supelec, 91192 Gif-sur-Yvette cedex, France
[4]Lab. De Mathématiques-UMR 6621 CNRS, Nice-Sophia Antipolis University, 06108 Nice cedex 2, France

In this work, we compare two nonconforming movement techniques: the mortar element method and the Lagrange multipliers. We present a unified formulation that can be easily used for electrical machines analysis. The anti-periodicity conditions as well as the use of high-order interface are discussed. The obtained linear systems are compared and results are shown for a permanent magnet machine.

Index Terms—**Hierarchic elements, Lagrange multipliers, mortar element method, movement.**

I. Introduction

THE TECHNIQUES based on Lagrange multipliers are very efficient to perform the movement, especially for electromotive force and torque evaluations, which are determinant to coupled or dynamic problems. This paper shows the way to obtain the final systems for mortar element method (MEM) [1], [2] and Lagrange multipliers method (LM) [3]. The aim of this work is to demonstrate that is possible to obtain the final system for MEM and for LM using the same matrices to couple the subdomains. We compare the final systems and the computational cost of the methods. In fact, the two methods produce the same results, but the final systems are different, and care must be taken to solve them. It is also verified that we can use high-order interface and anti-periodicity conditions with either MEM or LM.

II. Mortar Element Method

This work presents an MEM formulation called "constrained" because the coupling condition is applied directly to the discrete space. The MEM considers two subdomains that are connected by a sliding interface Γ.

The meshes of these subdomains are condensed independently as in the traditional finite-element method. One domain is considered the slave and the other the master. We choose the rotor as the master and stator as the slave. The vector potential at the nodes of the slave interface side $\mathbf{A}_s^\Gamma$ is a function of the master interface side $\mathbf{A}_m^\Gamma$. A brief introduction to the MEM can be found in [1], and it can be expressed by

$$\mathbf{A}_s^\Gamma = \mathbf{Q}\mathbf{A}_m^\Gamma \tag{1}$$

where

$$\mathbf{Q} = \mathbf{C}^{-1}\mathbf{D}. \tag{2}$$

$\mathbf{C}$ and $\mathbf{D}$ may be calculated by line integrals over Γ

$$\mathbf{C}(i,j) = \int_\Gamma \psi_i\psi_j d\Gamma \quad \mathbf{D}(i,j) = \int_\Gamma \varphi_j\psi_i d\Gamma. \tag{3}$$

The functions ψ_i and φ_i are the base functions of slave and master discretizations on node i, respectively. As the potentials at the nodes of the slave interface $\mathbf{A}_s^\Gamma$ are functions of the potentials on the master interface $\mathbf{A}_m^\Gamma$, they can be eliminated in the final system. The potentials over the whole domain, slave and master, can be linked as follows:

$$\begin{bmatrix} \mathbf{A}_s^\Gamma \\ \mathbf{A}_s \\ \mathbf{A}_m^\Gamma \\ \mathbf{A}_m \end{bmatrix} = \begin{bmatrix} \mathbf{0} & \mathbf{Q} & \mathbf{0} \\ \mathbf{Id} & \mathbf{0} & \mathbf{0} \\ \mathbf{0} & \mathbf{Id} & \mathbf{0} \\ \mathbf{0} & \mathbf{0} & \mathbf{Id} \end{bmatrix} \begin{bmatrix} \mathbf{A}_s \\ \mathbf{A}_m^\Gamma \\ \mathbf{A}_m \end{bmatrix} \tag{4}$$

which can be noted as

$$\mathbf{A} = \tilde{\mathbf{Q}}\bar{\mathbf{A}} \tag{5}$$

where $\tilde{\mathbf{Q}}$ is the coupling matrix, $\mathbf{Id}$ is the identity matrix, and $\mathbf{A}_s$ and $\mathbf{A}_m$ are the potentials out of the interface in the slave and master meshes, respectively.

Applying the coupling matrix on the original finite-element system $\mathbf{MA} = \mathbf{S}$, or

$$\begin{bmatrix} \mathbf{M}_s & \mathbf{0} \\ \mathbf{0} & \mathbf{M}_m \end{bmatrix} \cdot \begin{bmatrix} \mathbf{A}_s \\ \mathbf{A}_m \end{bmatrix} = \begin{bmatrix} \mathbf{S}_s \\ \mathbf{S}_m \end{bmatrix} \tag{6}$$

we have

$$\tilde{\mathbf{Q}}^T\mathbf{M}\tilde{\mathbf{Q}}\bar{A} = \tilde{\mathbf{Q}}^T\mathbf{S}. \tag{7}$$

$\mathbf{M}_s, \mathbf{M}_m, \mathbf{S_s}$, and $\mathbf{S}_m$ are the conventional stiffness matrices and load vectors of each domain.

The resultant system above is sparse and positive definite. So, it can be easily solved by iterative methods.

III. Lagrange Multipliers

A. Formulation

The whole domain is decomposed, as shown in Fig. 1, in two subdomains Ω_a and Ω_b connected by a sliding interface Γ.

One way to find the LM formulation is from the weak form of the magnetostatic field formulation [4]. The integration by parts is performed over each of the two subdomains Ω_a and Ω_b separated by the sliding interface Γ. As the flux integrals associated with the linked (anti)-periodicity boundaries $\partial\mathrm{P}_1$ and $\partial\mathrm{P}_2$ as well as the boundaries with Dirichlet conditions $\partial\mathrm{D}$ vanish,

Digital Object Identifier 10.1109/TMAG.2006.871431

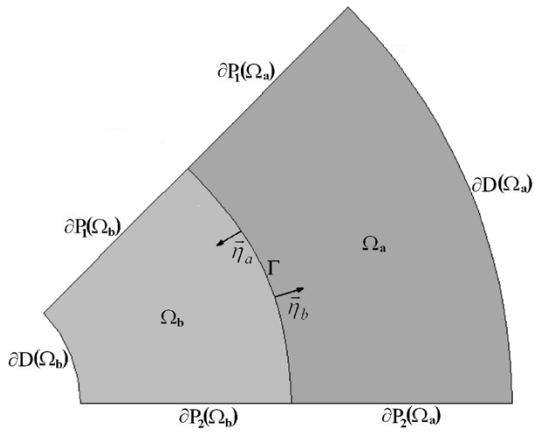

Fig. 1. Subdomains Ω_a and Ω_b separated by a sliding interface Γ.

only the flux integral associated with the interface Γ remains on the variational formulation

$$-\int_\Gamma v_a \frac{1}{\mu_a}\vec{\nabla}A_a\cdot\vec{\eta}_a d\Gamma+\int_{\Omega_a}\vec{\nabla}v_a\cdot\frac{1}{\mu_a}\vec{\nabla}A_a d\Omega_a = \int_{\Omega_a} v_a\left(J_a+\frac{\partial}{\partial x}\left[\frac{1}{\mu_a}B^a_{oy}\right]-\frac{\partial}{\partial y}\left[\frac{1}{\mu_a}B^a_{OX}\right]\right)d\Omega_a \quad (8)$$

$$-\int_\Gamma v_b \frac{1}{\mu_b}\vec{\nabla}A_b\cdot\vec{\eta}_b d\Gamma+\int_{\Omega_b}\vec{\nabla}v_b\cdot\frac{1}{\mu_b}\vec{\nabla}A_b d\Omega_b = \int_{\Omega_b} v_b\left(J_b+\frac{\partial}{\partial x}\left[\frac{1}{\mu_b}B^b_{oy}\right]-\frac{\partial}{\partial y}\left[\frac{1}{\mu_b}B^b_{OX}\right]\right)d\Omega_b. \quad (9)$$

In the equations above, v_a and v_b are test functions, J_a and J_b the current densities, and A_a and A_b the vector potentials in each domain. $B^a_{oy}, B^a_{OX}, B^b_{oy}$, and B^b_{OX} are remanent induction components and μ_a and μ_b the magnetic permeabilities. The terms $(1/\mu_a)\vec{\nabla}A_a\cdot\vec{\eta}_a$ and $(1/\mu_b)\vec{\nabla}A_b\cdot\vec{\eta}_b$ may be written as $(1/\mu_a)(\partial A_a/\partial\eta_a)$ and $(1/\mu_b)(\partial A_b/\partial\eta_b)$, which represent the tangential components of magnetic field on Γ. From the conservation of the tangential component of magnetic field on Γ, we have

$$\lambda=-\frac{1}{\mu_b}\frac{\partial A_a}{\partial\eta_a}=\frac{1}{\mu_b}\frac{\partial A_b}{\partial\eta_b}. \quad (10)$$

Using (10) on (8) and (9) we have

$$\int_\Gamma \lambda v_a d\Gamma+\int_{\Omega_a}\vec{\nabla}v_a\cdot\frac{1}{\mu_a}\vec{\nabla}A_a d\Omega_a = \int_{\Omega_a} v_a\left(J_a+\frac{\partial}{\partial x}\left[\frac{1}{\mu_a}B^a_{oy}\right]-\frac{\partial}{\partial y}\left[\frac{1}{\mu_a}B^a_{OX}\right]\right)d\Omega_a \quad (11)$$

$$-\int_\Gamma \lambda v_b d\Gamma+\int_{\Omega_b}\vec{\nabla}v_b\cdot\frac{1}{\mu_b}\vec{\nabla}A_b d\Omega_b = \int_{\Omega_b} v_b\left(J_b+\frac{\partial}{\partial x}\left[\frac{1}{\mu_b}B^b_{oy}\right]-\frac{\partial}{\partial y}\left[\frac{1}{\mu_b}B^b_{OX}\right]\right)d\Omega_b. \quad (12)$$

The continuity of the vector potential on the interface has not been ensured yet. It is imposed in weak sense by

$$\int_\Gamma (A_a-A_b)v_c d\Gamma=0. \quad (13)$$

Another way to find the equations (11)–(13) of the LM formulation is to minimize the energy functional associated with the magnetostatic problem [3], [4], [7]

$$\Pi=\int_{\Omega_a}\left(\int_0^{B_a}H_a dB_a-A_aJ_a\right)d\Omega_a+\int_{\Omega_b}\left(\int_0^{B_b}H_b dB_b-A_bJ_b\right)d\Omega_b \quad (14)$$

and, to ensure the continuity of A at the interface Γ, a new functional is added

$$\Pi^*=\int_\Gamma\lambda(A_a-A_b)d\Gamma \quad (15)$$

where λ is the Lagrange multiplier. With the first variation of $\Pi+\Pi^*$, exactly the same equations are obtained and the Lagrange multiplier λ is identified again as the tangential component of the magnetic field on Γ [3].

B. Discretization

We apply the classical nodal approximation for the vector potential as $A_{ah}=\sum_{i=1}^{m_a}N_i^aA_i^a$ and $A_{bh}=\sum_{i=1}^{m_b}N_i^bA_i^b$, where m_a and m_b are the number of nodes of the discretizations of the subdomains Ω_a and Ω_b. N_i^a and N_i^b are the approximation base functions of node i. If the numbering of nodes in each domain is made such that that those belonging to the interface Γ take the first places and if the same discrete space of the approximated solution A_{ah} in Ω_a is used to the discretization of the Lagrange multiplier λ (as its support is only in the interface Γ of Ω_a), we have

$$\lambda_h=\sum_{j=1}^{m_a^\Gamma}N_j^a\big|_\Gamma\lambda_j\quad j\in\Gamma(\Omega_a) \quad (16)$$

where $N_j^a|_\Gamma$ is the trace of N_j^a on Γ and m_a^Γ is the number of nodes belonging to $\Gamma(\Omega_a)$. For the approximation of the test function on Ω_a we have

$$v_{ah}=N_i^a\quad i\in\Omega_a. \quad (17)$$

Using (16) and (17) on the first term of (11)

$$\int_\Gamma\lambda_h v_{ah}d\Gamma=\sum_{j=1}^{m_a^\Gamma}\int_\Gamma N_i^a\big|_\Gamma N_j^a\big|_\Gamma d\Gamma\lambda_j i\in\Omega_a,\quad j\in\Gamma(\Omega_a) \quad (18)$$

or

$$\mathbf{G}^T\bar{\boldsymbol{\lambda}} \quad (19)$$

where

$$\mathbf{G}^T(i,j)=\int_\Gamma N_i^a\big|_\Gamma N_j^a\big|_\Gamma d\Gamma,\quad i\in\Omega_a,\ j\in\Gamma(\Omega_a) \quad (20)$$

and $\bar{\boldsymbol{\lambda}}$ is a set of m_a^Γ Lagrange multipliers λ_j. For $i>m_a^\Gamma$, the functions $N_i^a|_\Gamma$ vanish at Γ, because they do not belong to it. We can then write

$$\mathbf{G}^T=\begin{bmatrix}\mathbf{C}^T\\ \mathbf{O}\end{bmatrix} \quad (21)$$

where $\mathbf{C}^T$ is a $m_a^\Gamma \times m_a^\Gamma$ matrix with

$$\mathbf{C}^T(i,j)=\int_\Gamma N_i^a \left|_\Gamma N_j^a\right|_\Gamma d\Gamma, \quad i \in \Gamma(\Omega_\mathrm{a}),\ j \in \Gamma(\Omega_\mathrm{a}). \tag{22}$$

For the approximation of the test function on Ω_b, we have

$$v_{bh} = N_i^b \quad i \in \Omega_\mathrm{b}. \tag{23}$$

Using (16) and (23) on the first term of (12)

$$\int_\Gamma \lambda_h v_{bh} d\Gamma = \sum_{j=1}^{m_a^\Gamma} \int_\Gamma N_i^b \left|_\Gamma N_j^a\right|_\Gamma d\Gamma \lambda_j, \quad i \in \Omega_\mathrm{b},\ j \in \Gamma(\Omega_\mathrm{a}) \tag{24}$$

or

$$\mathbf{H}^T \bar{\boldsymbol{\lambda}} \tag{25}$$

where

$$\mathbf{H}^T(i,j) = \int_\Gamma N_i^b \left|_\Gamma N_j^a\right|_\Gamma d\Gamma \quad i \in \Omega_\mathrm{b}, \quad j \in \Gamma(\Omega_\mathrm{a}). \tag{26}$$

As $N_i^b|_\Gamma$ is zero for $i > m_b^\Gamma$, where m_b^Γ is the number of nodes belonging to $\Gamma(\Omega_\mathrm{b})$

$$\mathbf{H}^T = \begin{bmatrix} \mathbf{D}^T \\ \mathbf{0} \end{bmatrix} \tag{27}$$

where $\mathbf{D}^T$ is a $m_b^\Gamma \times m_a^\Gamma$ matrix with

$$\mathbf{D}^T(i,j)=\int_\Gamma N_i^b \left|_\Gamma N_j^a\right|_\Gamma d\Gamma, \quad i \in \Gamma(\Omega_\mathrm{b}),\ j \in \Gamma(\Omega_\mathrm{a}). \tag{28}$$

If the same approximation of the Lagrange multiplier λ_h in (16) is used to the discretization of the test function v_c on (13), as shown in [4]–[6], we have

$$v_{ch} = N_i^a|_\Gamma, \quad i \in \Gamma(\Omega_\mathrm{a}). \tag{29}$$

Using (29) and the vector potential approximation A_{ah} on the first term of (13)

$$\int_\Gamma A_{ah} v_{ch} d\Gamma = \sum_{j=1}^{m_a} \int_\Gamma N_i^a \left|_\Gamma N_j^a\right|_\Gamma d\Gamma A_j^a, \quad i \in \Gamma(\Omega_\mathrm{a}),\ j \in \Omega_\mathrm{a} \tag{30}$$

or

$$\mathbf{G}\bar{\mathbf{A}}_a \tag{31}$$

where

$$\mathbf{G}(i,j) = \int_\Gamma N_i^a \left|_\Gamma N_j^a\right|_\Gamma d\Gamma, \quad i \in \Gamma(\Omega_\mathrm{a}),\ j \in \Omega_a \tag{32}$$

as $N_j^a|_\Gamma$ is zero for $j > m_a^\Gamma$

$$\mathbf{G} = [\mathbf{C} \quad \mathbf{0}] \tag{33}$$

where $\mathbf{C}$ is a $m_a^\Gamma \times m_a^\Gamma$ matrix with

$$\mathbf{C}(i,j)=\int_\Gamma N_i^a \left|_\Gamma N_j^a\right|_\Gamma d\Gamma, \quad i \in \Gamma(\Omega_\mathrm{a}),\ j \in \Gamma(\Omega_\mathrm{a}). \tag{34}$$

In the same way, for the second term of (13), we have

$$\int_\Gamma A_{bh} v_{ch} d\Gamma = \sum_{j=1}^{m_b} \int_\Gamma N_i^a \left|_\Gamma N_j^b\right|_\Gamma d\Gamma A_j^b, \quad i \in \Gamma(\Omega_\mathrm{a}),\ j \in \Omega_\mathrm{b} \tag{35}$$

or

$$\mathbf{H}\bar{\mathbf{A}}_b \tag{36}$$

where

$$\mathbf{H}(i,j) = \int_\Gamma N_i^a \left|_\Gamma N_j^b\right|_\Gamma d\Gamma, \quad i \in \Gamma(\Omega_\mathrm{a}),\ j \in \Omega_\mathrm{b} \tag{37}$$

as $N_j^b|_\Gamma$ is zero for $j > m_b^\Gamma$

$$\mathbf{H} = [\mathbf{D} \quad \mathbf{0}] \tag{38}$$

where $\mathbf{D}$ is a $m_a^\Gamma \times m_b^\Gamma$ matrix with

$$\mathbf{D}(i,j)=\int_\Gamma N_i^a \left|_\Gamma N_j^b\right|_\Gamma d\Gamma, \quad i \in \Gamma(\Omega_\mathrm{a}),\ j \in \Gamma(\Omega_\mathrm{b}). \tag{39}$$

Finally, the following symmetric system is obtained:

$$\begin{bmatrix} \mathbf{M}_a & \vdots & \mathbf{0} & \vdots & \mathbf{C}^T \\ & & & & \mathbf{0} \\ \cdots & \cdots & \cdots & \cdots & \cdots \\ \mathbf{0} & \vdots & \mathbf{M}_b & \vdots & -\mathbf{D}^T \\ & & & & \mathbf{0} \\ \cdots & \cdots & \cdots & \cdots & \cdots \\ \mathbf{C} \quad \mathbf{0} & \vdots & -\mathbf{D} \quad \mathbf{0} & \vdots & \mathbf{0} \end{bmatrix} \begin{bmatrix} \bar{\mathbf{A}}_a^\Gamma \\ \bar{\mathbf{A}}_a^o \\ \cdots \\ \bar{\mathbf{A}}_b^\Gamma \\ \bar{\mathbf{A}}_b^o \\ \cdots \\ \bar{\boldsymbol{\lambda}} \end{bmatrix} = \begin{bmatrix} \mathbf{S}_a \\ \cdots \\ \mathbf{S}_b \\ \cdots \\ \mathbf{0} \end{bmatrix} \tag{40}$$

where $\mathbf{M_a}, \mathbf{M_b}, \mathbf{S_a}$, and $\mathbf{S_b}$ are the conventional stiffness matrices and load vectors of each domain. While $\bar{\mathbf{A}}_\mathrm{a}^\Gamma$ and $\bar{\mathbf{A}}_b^\Gamma$ are the potentials on $\Gamma(\Omega_\mathrm{a})$ and $\Gamma(\Omega_\mathrm{b})$, $\bar{\mathbf{A}}_a^o$ and $\bar{\mathbf{A}}_b^o$ are the ones out of Γ in Ω_a and Ω_b. The system (40) is ill conditioned and nonpositive definite.

It is clear at this point that, if we consider Ω_a as slave and Ω_b as master, the integrals (34) and (39) are identical to (3), because over Γ ψ_i and φ_i in the MEM are defined exactly as $N_i^a|_\Gamma$ and $N_i^b|_\Gamma$ in the LM. They are 1 on the node i and zero on the other nodes of the interface Γ, i.e., they are traditional finite-element functions defined over Γ. That is, we use the same discrete space on Γ for either MEM and LM. Thus, the matrices $\mathbf{C}$ and $\mathbf{D}$ in (34) and (39) are identical to (3). This means that we can construct these matrices as shown in [2] for first-, second-, or third-order hierarchic interpolation on Γ. In other words, if we construct the matrices $\mathbf{C}$ and $\mathbf{D}$, we can use them with either MEM in the "constrained" form, applying the transformation on (7), or LM using the system (40).

C. MEM From the LM Formulation

From the last line of (40) we have

$$\bar{\mathbf{A}}_a^\Gamma = \mathbf{C}^{-1}\mathbf{D}\bar{\mathbf{A}}_b^\Gamma. \tag{41}$$

If we call Ω_a as slave, because the potentials on $\Gamma(\Omega_\mathrm{a})$ are functions of the potentials on $\Gamma(\Omega_\mathrm{b})$, and Ω_b as master, we have exactly the mortar condition expressed in (1). The potentials at the nodes of the slave interface $\Gamma(\Omega_\mathrm{a})$ are then eliminated in the final system as shown in Section II. Reference [8] shows

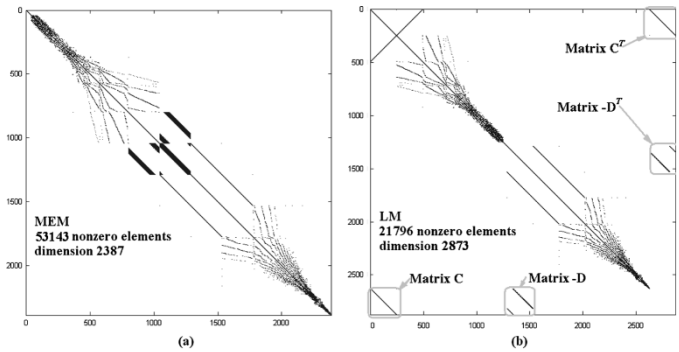

Fig. 2. View of nonzero elements for (a) MEM and (b) LM methods. Mesh 3.

TABLE I
COMPUTATION TIME

	mesh 1	mesh 2	mesh 3
Total number of nodes	930	1688	2630
Computation Time[s] MEM/ICCG	.31	.47	.69
Computation Time[s] LM/Gauss	.25	1.67	6.9

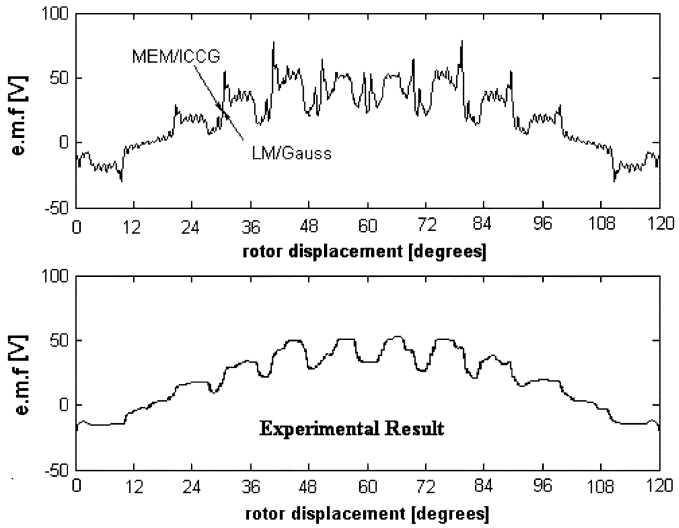

Fig. 3. Electromotive force for mesh 1.

a similar equivalent MEM formulation for a harmonic sliding interface technique.

IV. Results and Discussion

The resultant systems shown in Fig. 2 are for a permanent magnet machine (mesh 3 in Table I) with the rotor at 20.5 degrees (nonconforming position). We can observe that even with the small system dimension the MEM has more than two times more nonzero elements than LM. However, the resultant matrix for MEM is positive definite and may be solved by an iterative method like ICCG. The system for LM is ill conditioned (the condition number is of order 10^{+20}) and is nonpositive definite (it has negative eigenvalues). So, it cannot be solved by ICCG. We can obtain the convergence with the biconjugate gradients method and minimum residual method (which are faster than the other tested methods like generalized minimum residual method and symmetric LQ method), but they still need about 7000 iterations. So the Gaussian elimination method is used. Table I shows that for meshes with more than about 1000 nodes, MEM with ICCG becomes faster than LM with Gaussian elimination. The inversion of matrix $\mathbf{C}$, necessary to apply the MEM, demands an insignificant time, compared with the system solution, because the matrix is diagonal, symmetric, and sparse (Fig. 2).

The electromotive force (e.m.f.) calculation is appropriate to show the convergence of the two methods because a little difference on the potential vector may affect the e.m.f., since it is calculated by time derivatives. According our tests, the vector potential results for MEM/ICCG are identical to those obtained with LM/Gaussian elimination until about the seventh decimal digit for a tolerance of 1e-6 for ICCG. This is sufficiently accurate to produce the same e.m.f. (Fig. 3) and torque results for both methods. As expected, MEM and LM produce exactly the same results when using Gaussian elimination.

V. Conclusion

This work demonstrates that is possible to obtain the final system for MEM and for LM using the same matrices to couple the subdomains. We can use high-order interface and anti-periodicity conditions with either MEM or LM. They produce the same results, but the final equation systems are different. MEM produces a sparse and positive definite matrix and may be solved by ICCG, while LM has an ill conditioned and nonpositive definite system that, according our tests, is better handled by a direct method. MEM is faster than LM when the system dimension increases.

References

[1] M. Taferguenit, L. Santandrea, F. Rapetti, F. Bouillault, and M. Gabsi, "Two methods to take into account the movement within a finite element modelization of an electrical device," in *Eur. Symp. Num. Meth. Electromagn. (JEE)*, Toulouse, France, Mar. 2002, pp. 19–24.

[2] O. J. Antunes, J. P. A. Bastos, N. Sadowski, A. Razek, L. Santandrea, F. Bouillault, and F. Rapetti, "Using high-order interpolation with mortar element method for electrical machines analysis," *IEEE Trans. Magn.*, vol. 41, no. 5, pp. 1472–1475, May 2005.

[3] D. Rodger, H. C. Lai, and P. J. Leonard, "Coupled elements for problems involving movement," *IEEE Trans. Magn.*, vol. 26, no. 2, pp. 548–55, Mar. 1990.

[4] N. Gasmi, "Contribuition à la Modélization des phénomènes Électriques-magnétiques couplés et du mouvement pour les systèmes électromagnétiques en 3D," Thèse de Doctorat, l'Université de Paris 6, Oct. 1996.

[5] H. C. Lai, D. Rodger, and P. C. Coles, "A finite element scheme for colliding meshes," *IEEE Trans. Magn.*, vol. 35, no. 3, pp. 1362–1364, May 1999.

[6] P. J. Leonard, H. C. Lai, G. Hainsworth, D. Rodger, and J. F. Eastham, "Analysis of the performance of tubular pulsed coil induction launchers," *IEEE Trans. Magn.*, vol. 29, no. 1, pp. 686–690, Jan. 1993.

[7] Y. Marechal, G. Meunier, J. L. Coulomb, and H. Magnin, "A general purpose tool for restoring inter-element continuity," *IEEE Trans. Magn.*, vol. 28, no. 2, pp. 1728–1731, Mar. 1992.

[8] H. De Gersem and T. Weiland, "Harmonic weighting functions at the sliding interface of a finite-element machine model incorporating angular displacement," *IEEE Trans. Magn.*, vol. 40, no. 2, pp. 545–548, Mar. 2004.

Manuscript received June 28, 2005 (e-mail: orlando@grucad.ufsc.br).